Journal of Aviation/Aerospace Education & Research

Volume 29
Number 1 *JAAER 2020*

Article 5

2020

Design, Construction and Testing of a 3-Component Force Balance for Educational Wind Tunnels in Undergraduate Aerodynamics

Milan Tomin
Queens University of Charlotte, milantomin.ns@gmail.com

Marco Scipioni
Queens University of Charlotte, scipionim@queens.edu

Benjamin Gatti
Queens University of Charlotte, benjamingatti@gmail.com

Introduction

Since the Wright Brothers' first flight in 1903, the knowledge of how airplanes fly has increased significantly. Most scientific progress in the airplane industry has been in safety, fuel efficiency, and in achieving higher economic performance. Ribeiro et al. (2007) said that "most modern civil jet aircrafts are about 70% more fuel-efficient per passenger-km than 40 years ago." Furthermore, an additional 40-50% progress in fuel efficiency is expected by 2050 (Ribero et al., 2007). Much of the improvements come from wing aerodynamics as well as engine efficiency. Much of the improvements come from wing aerodynamics as well as engine efficiency. However, while enhancing wing efficiency, aerospace engineers started introducing higher design complexity, and, after the 1990s, their focus shifted to simpler, yet still efficient designs. For example, airplanes with three-slotted wings were later replaced by airplanes with simple single-slotted wings (Anderson & Eberhardt, 2010). To investigate and study aerodynamics of a specific airplane design, its aerodynamic components and devices are generally tested on scale models placed inside a wind tunnel to experimentally predict and extrapolate the aerodynamic performance of the life size-models. Building a custom wind tunnel and equipping it with a force balance to capture aerodynamic data is a great learning experience for students seeking a deeper understanding of the core principles of lift, drag, aerodynamic movement, and airfoil design.

Smaller universities and colleges not offering aerospace engineering do not have the appropriate facilities and equipment for studying aerodynamics. To overcome this limitation, this article presents the novel design, construction, and testing of a 3-component force balance specifically intended for educational aerodynamics. The work presented in this article is meant to facilitate the experience of building a force balance through a step-by-step guide for students interested in wind tunnel experimentation. Reynolds indicated that performing wind tunnel testing in the lab had a lasting and significant impact on his aviation, non-engineering undergraduate students (Reynolds, 2005). The force balance, which is a fundamental part of any wind tunnel testing, allows students to conduct force and moment measurements and learn from their graphical visualization. Rigby's study included simulations in the instructional plan which can lead to improvement in students' performance in aerodynamics and applied aerodynamics (Rigby, 2015). Hands-on learning through wind tunnel experiments can improve the students' theoretical knowledge and provide them with an opportunity to analyze the aerodynamic forces measured by the force balance. In regards to the force balance presented in this article, the main requirements were to be a) to be inexpensive, b) being easy to build with simple tools, and c) being easy to replicate, which will allow students from universities without an aerodynamic research lab to build a force balance from scratch. Project-based learning is engaging, and it empowers students to develop technical intuition, gain a deeper understanding of aerodynamic forces, and become passionate about aerodynamics in general.

A sophisticated force balance is capable of measuring drag forces with 0.001% accuracy and lift forces with 0.1% accuracy (Advisory Group for Aerospace Research & Development [AGARD], 1992). The force balance described in this work has an accuracy limited to 10% for both the drag and the lift forces but, at the same time, is easily buildable using basic materials and electronics. The main force balance components were three load cells, a servo motor, and the acrylic frame. Once built, the force balance is capable of measuring lift, drag, pitching moment about the leading edge, as well as their coefficients, and the position of the center of pressure. To test the force balance and validate its measurements, the authors built a low-Reynolds number wind tunnel from the ground up (a test section of 144 in^2 squared cross-

DOI: https://doi.org/10.15394/jaaer.2020.1809

sectional area, contraction ratio of 9, a nozzle with a constant 12° expansion angle, a diffuser with constant 4° expansion angle and 256 in^2 square cross-sectional area). A data collection example is also included and explained in the article.

Materials and Methods

Components

The main components of this external force balance are shown in Table 1.

Table 1

Components Used to Build the Force Balance

Part Name	Make	Model	Amazon SKU
Servo motor	Hitec RDC Inc.	33485S Deluxe HS-485HB	B002HPUKS8
load cells (5kg)	Phoncoo	5KG Digital Load Cell Weight Sensor	B07JWC85SN
load cell (1kg)	Phoncoo	Digital Load Cell Weight Sensor 1KG	B07JGJWY8L
HX711 amplifiers	FOR-Arduino	HX711 Weighing Sensor Module - Green	B07DWBDW2K
Arduino Nano	Arduino	A000005	B0097AU5OU

Load cells. The thesis presented by Pravin Vadassery indicates that, in the case of internal and external force balances, strain gauges, piezoelectric films, and accelerometers are commonly used techniques for measuring forces in a wind tunnel (Vadassery, 2012). Additionally, in the same research, it is stated that Robinson, Schramm, and Hannemann (2007) found that external force balance shows to be more accurate; therefore, the authors decided to make an external force balance, which seemed easier to manufacture (Robinson et al., 2007). Two 5-kg load cells were used to measure lift and pitching moment while a 1-kg load cell was used to measure drag. The load cells were selected on the advice of Gary Eaker – designer and founder of Aerodyn wind tunnel which is used by numerous NASCAR teams (G. Eaker, personal communication, February 11, 2018). Based on lecture notes from Brown University, load cells can be used for precise force measuring (Bower & Xu, 2019).

A load cell is a transducer converting a mechanical force into an electrical signal by means of four metallic strain gauges interconnected to form a Wheatstone bridge. When a force is applied to one load cell, the strain gauges' electrical resistance changes in proportion to the experienced strain. Subsequently, the Wheatstone bridge outputs a signal that is proportional to the externally applied force.

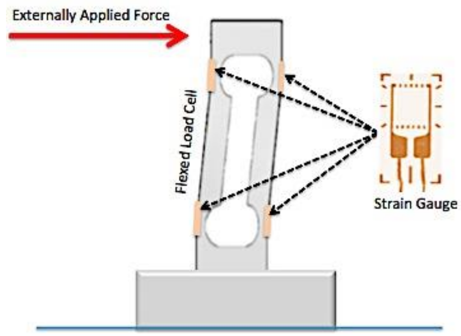

Figure 1. Load cell and its four strain gauges forming a Wheatstone bridge to measure applied loads.

Servo motor. The force balance includes a servo motor. The servo horn, which attaches to the motor's shaft, is connected to the tested wing profile through thin and stiff piano wires to control and adjust the wing's angle of attack (AoA). Since the servo horn rotation is not linearly correlated with the wing's AoA, a simple calibration procedure with a high-precision digital level is required to correctly map the AoA with the servo horn rotation.

DOI: https://doi.org/10.15394/jaaer.2020.1809

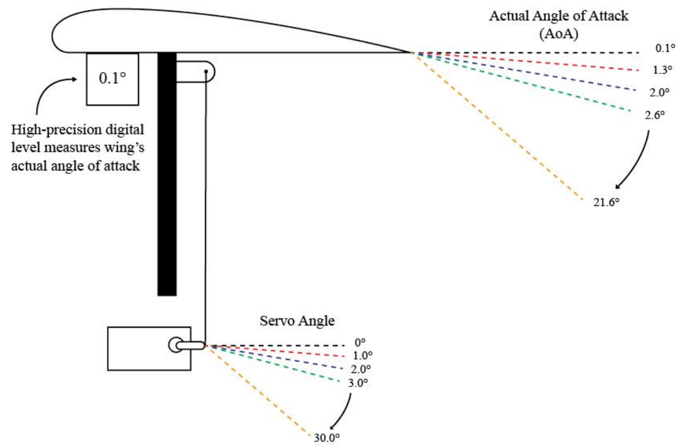

Servo Angle	0°	1.0°	2.0°	3.0°	...	30.0°
Actual Angle of Attack (AoA)	0.1°	1.3°	2.0°	2.6°	...	21.6°

Figure 2. Angle calibration using high precision digital level.

Custom circuit board. The aerodynamic forces exerted on the tested wing model are transformed by the load cells into electrical signals which are sent to an Arduino Nano microcontroller connected to a computer for data collection and analysis. A custom design circuit board was fabricated to interconnect the three load cells and their HX711 amplifiers to the Arduino Nano microcontroller. According to González et al. (2011), amplifiers are an indispensable component of the force balance as they increase the analog signal output produced by the load cells and convert it into a digital form (Gonzalez et al., 2011).

Apart from minor modifications, additions, and corrections by the authors, most of the Arduino code was written by Itziar Bueno Tintoré and is available in her bachelor's thesis at University of Zagreb (Bueno Tintoré, 2018). In her thesis, Bueno Tintoré uses Arduino Uno instead of a custom circuit board with Arduino Nano, like the authors of this article did. Yet other microcontroller options are surely viable. The corresponding author encourages readers interested in the full code to contact him directly via email. The code controls the servo motor, allowing it to maintain a fixed position or sweep through different positions at a predetermined speed. After successfully uploading the code on the Arduino microcontroller, the three load cells must be calibrated using known weights to find the suitable calibration constant to produce accurate force balance measurements. The determination of the calibration constant involves placing known weights on each of the load cells and adjusting the calibration constant until the measured weight output from the Arduino matches the applied weight. Each load cell has a different calibration constant to account for. More detailed information on calibration is provided in the code.

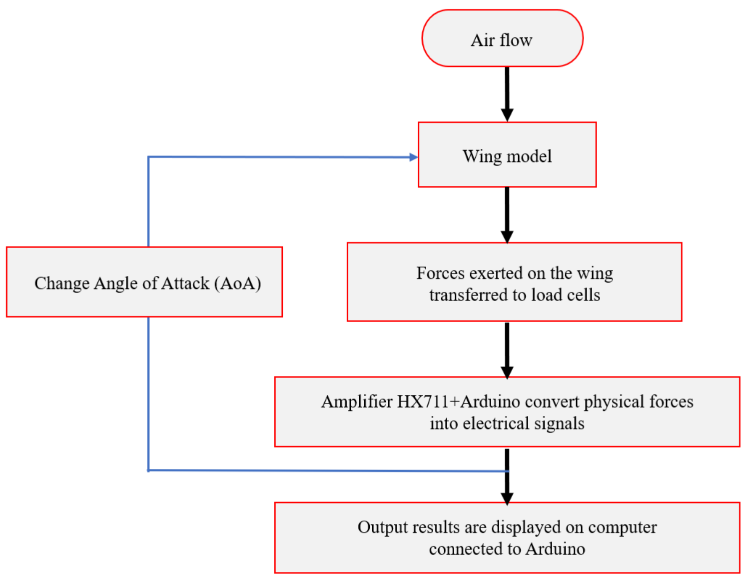

Figure 3. Flow chart showing the basic principle how the force balance functions.

Supplies

The force balance assembly was built using basic materials such as clear acrylic with one-quarter of an inch thickness, aluminum, carbon fiber, foam, small springs, and piano strings. The acrylic frame components, cut with a laser cutter, are sufficiently rigid to resist any bending caused by the aerodynamic forces acting on the wing, thus allowing force transfer to the load

DOI: https://doi.org/10.15394/jaaer.2020.1809

cells with minimal losses. The acrylic parts connecting the wing and the servo motor to the force balance assembly were created out of a one-sixteenth of an inch-inch thickness aluminum sheet. Connectors for the wing support were additionally strengthened using thin carbon fiber strips. The vertical carbon fiber strips supporting the wing are also sufficiently rigid to avoid bending under the horizontal drag force to be able to transmit the physical forces acting on the wing model to the respective load cells located in the assembly. The strips were positioned to create the least amount of drag, hence causing a smaller error in the collected data. Post and Morris (2010) warn that the force balance support structure can impact model's aerodynamics (Post & Morris, 2010). The wing model, made of foam, was cut using a hot wire, smoothened using sandpaper, and finally covered with a thin balsa wood sheeting.

Table 2

Acrylic Parts Used for Constructing the Force Balance

Part No.	Part Name
1	Bottom plate
2	Top plate
3	Top and bottom plate connector, rod and drag load cell holder
4	Top and bottom plate connector and rod holder
5	Middle section connector and drag load cell holder
6	Middle section and load cell spacers
7	Middle section connector and rod holder
8	Top plate (middle section)
9	Bottom plate (middle section)
10	Side connectors and load cell spacers
11	Bottom stand

Construction Steps

The force balance frame was created using acrylic components. All parts used for the construction are listed in the Table 2 and shown in the Figure 4 are available at a local hardware store. The dimensions of the acrylic parts depend on size of the load cells and on the size of the wind tunnel's test section where the force balance is positioned.

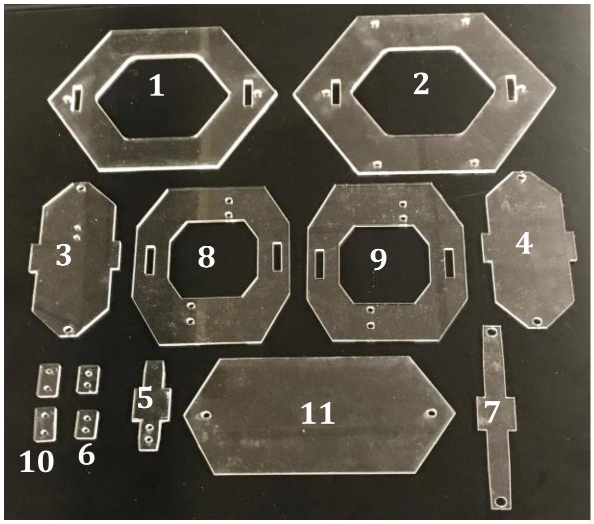

Figure 4. Acrylic frame components necessary to build the force balance.

Step 1. The first step in the construction process consisted of interconnecting part 1, part 3, and part 4. The first load cell was attached to part 3 using part 6 as a spacer. This load cell measures the horizontal drag force and must be oriented so that its 1-kg mark points in the same direction as the flow of air.

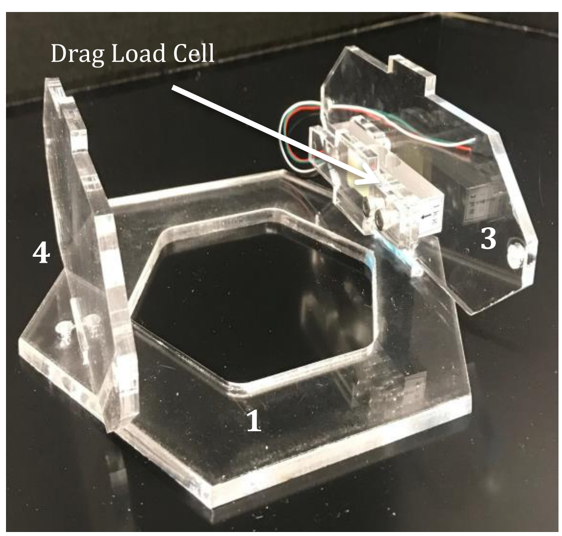

Figure 5. Part 5 attaches to the drag load cell which connects to part 3.

Step 2. The middle section of the force balance was created by interconnecting the hexagonal parts 8 and 9 using part 7 and two aluminum rods. The second load cell – the first for measuring lift – was attached to part 8 with the 5-kg mark pointing upward. This load cell will eventually attach to the servo motor used to control the wing's angle of attack. This configuration does not constrain the entire drag load cell, allowing one of its ends to be pulled to measure the horizontal drag force acting on the test wing. The middle section (part 7, part 8, part 9), which connects to the test wing model, can slide and experience a pull force which is transferred to part 5 fixed to the drag load cell.

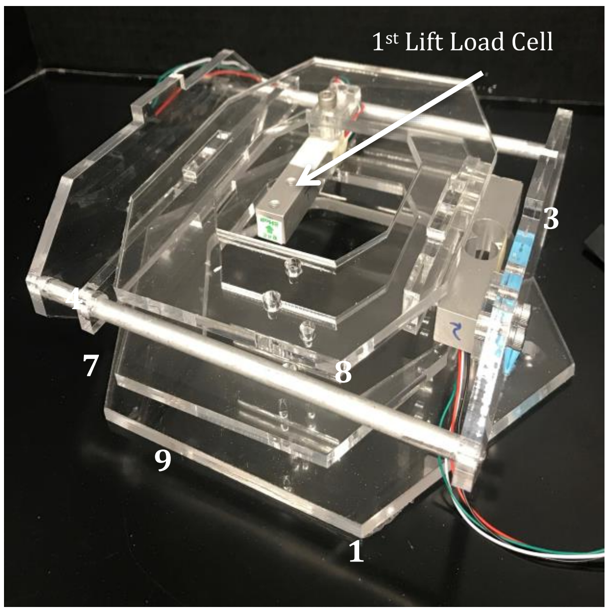

Figure 6. Middle section consists of parts 8 and 9 which serve as a housing for two lift load cells.

Step 3. The third construction step involves assembling the wing support structure (Figure 7) which includes two thin vertical carbon fiber strips, the third load cell – the second load cell intended to measure lift – and two aluminum connectors. The top connector serves to connect the test wing to the force balance while the bottom connector attached the load cell to the carbon strips. The arrow mark of the third load cell should also point upward. The wing support structure is then connected through the third load cell to part 8 using part 10 as a spacer.

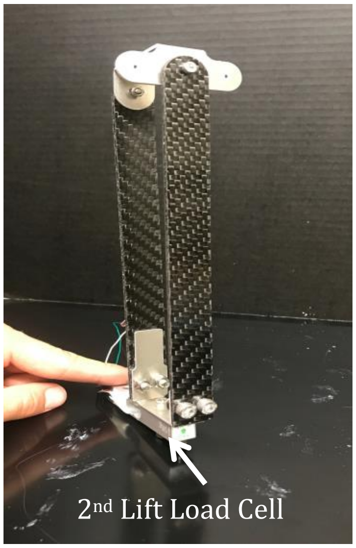

Figure 7. Test wing support structure was installed on the 2nd lift load cell before the load cell was positioned into place.

Step 4. This last construction step incorporates the servo motor and the custom circuit board into the force balance. The servo motor, which controls the wing's angle of attack, is fixed to the second lift load cell using an aluminum connector while the servo motor horn connects to the top part of the wing support structure via a piano string. The sum of the forces measured by the first and second lift load cells provides the net lift experienced by the test wing. In addition, the two vertical forces can be used to calculate the pitching moment.

The total lift force **L** acting on the wing is given by the vector sum of the two vertical forces $\mathbf{F_1}$ and $\mathbf{F_2}$ acting on the wing and measured by load cell 1 and load cell 2 respectively:

$$\boldsymbol{L} = \boldsymbol{F_1} + \boldsymbol{F_2}$$

The pitching moment $\mathbf{M_{LE}}$ about the leading edge (LE) is calculated as the vector sum of the moments $\mathbf{M_1}$ and $\mathbf{M_2}$ about the leading edge due to the forces $\mathbf{F_1}$ and $\mathbf{F_2}$:

$$\boldsymbol{M_{LE}} = \boldsymbol{M_1} + \boldsymbol{M_2} = \boldsymbol{x_1} \times \boldsymbol{F_1} + \boldsymbol{x_2} \times \boldsymbol{F_2}$$

where

$\boldsymbol{x}_1$ = vectorial distance between LE and $\boldsymbol{F}_1$

$\boldsymbol{x}_2$ = vectorial distance between LE and $\boldsymbol{F}_2$

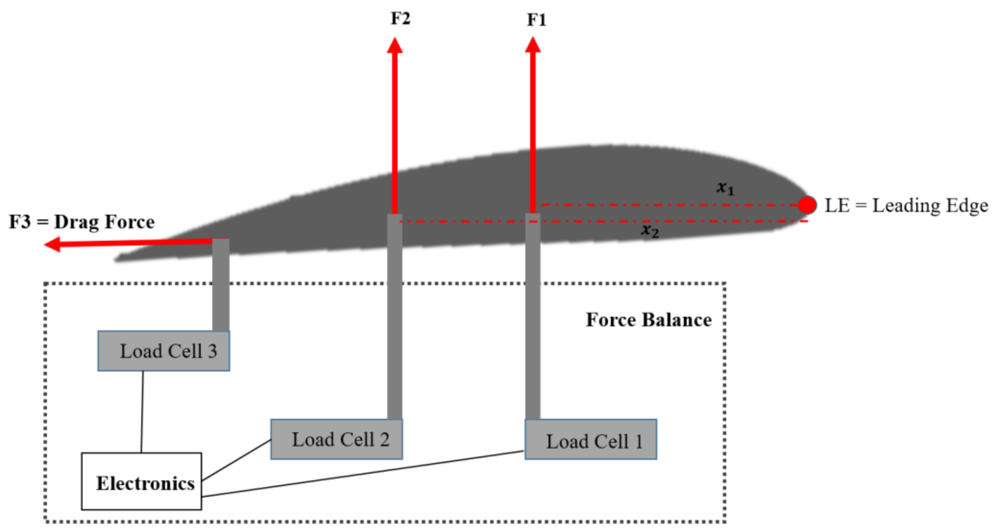

Figure 8. Schematic diagram of the force balance system and force measurement technique.

The hexagonal part 11, which attaches to the bottom of the force balances, serves as a platform to support the circuit board hosting the microcontroller.

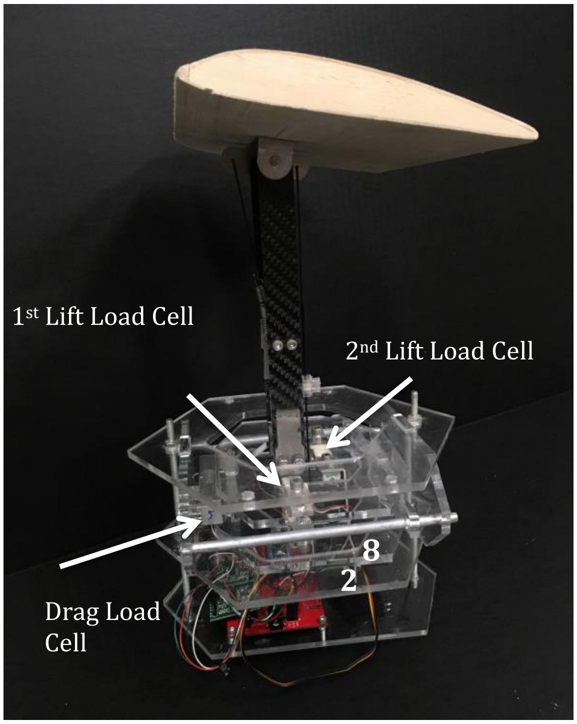

Figure 9. The Force Balance before it was mounted onto the wind tunnel test section.

Discussion

After all the steps from the previous section are completed, the force balance can be attached to a wind tunnel. Additionally, a wing model can be mounted on the force balance to test its aerodynamic properties. Although testing is not the focus of this article, an example of data collection and analysis is included to show how data can be visualized and to inspire further research.

Before testing, however, it is important to consider possible sources of error that can affect the experimental results, like the internal friction between the force balance components, noise fluctuations in the electronics, and an inaccurate calibration of the load cells. For example, the friction between internal components along the horizontal direction can cause inaccurate measurements of the drag force. Ideally, the friction between aluminum rods and the acrylic frame should be minimized as much as possible to remove any mechanical constraint on the wing model. Another important and possible source of error would be the onset of vibrations on the wing model due to high turbulence generated around it at high angle of attack. Vibrations are highly dependent on the wind speed and can also lead to inconsistent drag and lift measurement.

Force Balance Test Set-Up

The purpose of Part 2 in Figure 4 is to join the force balance apparatus to the bottom of the wind tunnel test section. The portion of the force balance including the load cells and electronics is hosted under the test section to minimize interference with the airflow and not compromise the quality of the collected data.

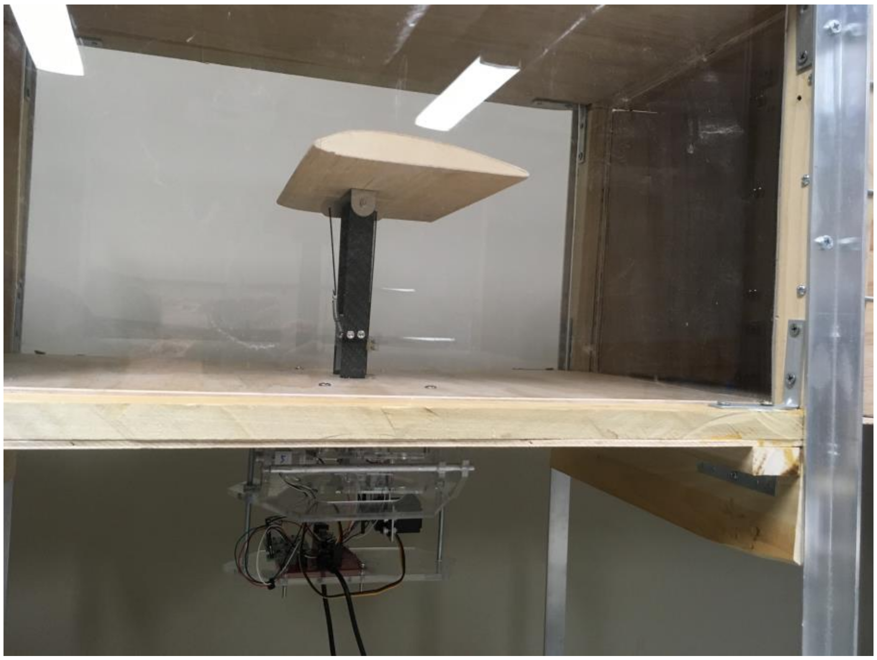

Figure 10. Force Balance when installed below the test section of an educational wind tunnel.

Data Collection Example

After the force balance was fully assembled and calibrated, the authors performed a basic aerodynamics test. The tested wing model was NACA 6412 foam wing having a 150 mm cord length and covered with balsa wood. The airflow speed, measured with a Vernier spirometer, was approximately 12 m/s and was produced using a 1HP 5000CFM fan. The wing's angle of attack (AoA), calibrated per procedure presented in the Figure 2, varied every 2 seconds from 0.1° up to 21.6°. In the code, the swept angular range for the AoA corresponded to the servo horn sweeping rotating from 0° to 30°, respectively. For each different AoA, a total of 19 points were collected and later averaged into a single value. The force balance data was output through the Arduino's serial port monitor and later imported into Matlab for data analysis and visualization.

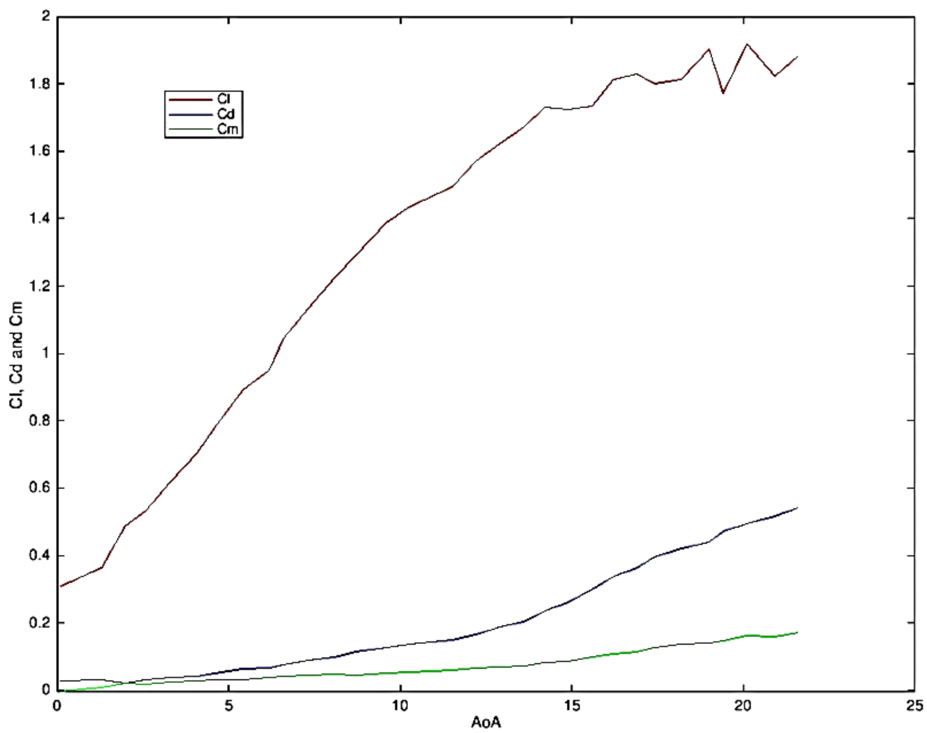

Figure 91. Angle of attack (AoA) on x-axis was independent variable while the two dependent variables were Lift coefficient (C_l) in red and Drag coefficient (C_d) in blue and Pitching moment in green (C_m).

The graph shows that as the angle of attack (AoA) increases, the lift coefficient (C_l), the drag coefficient (C_d) and the pitching moment (C_m) increase. It is interesting to note the behavior of the lift coefficient at around 15^0 which suggests that wing is approaching stall condition.

https://commons.erau.edu/jaaer/vol29/iss1/5
DOI: https://doi.org/10.15394/jaaer.2020.1809

Conclusion and Future Work

The work presented in this article provides a clear step-by-step procedure on how to construct a force balance for educational purposes. The described force balance can be manufactured with inexpensive components – a few load cells, a servo motor, and simple electronics.

The authors' future work will focus on a) using the force balance and wind tunnel to test different airfoil profiles and on b) expanding the system capabilities to be able to measure the air pressure distribution around the tested wing and visualize the flow streaklines through dye injection. This experimental apparatus has the potential to be used for undergraduate level study of other interesting phenomena like animal flight aerodynamics, turbulence, etc.

Acknowledgements

The authors would like to thank the Noble Fellowship at Queens University of Charlotte for the support as well as Enventys Partners LLC for providing tools and guidance throughout this project.

References

Advisory Group for Aerospace Research & Development (AGARD). (1992, January). *Special course on engineering methods in aerodynamic analysis and design of aircraft (R-783).* Neuilly-sur-Seine, France: North Atlantic Treaty Organization (NATO). Retrieved from https://www.sto.nato.int/publications/AGARD/Forms/AGARD Document Set/docsethomepage.aspx?ID=7464&FolderCTID=0x0120D5200078F9E87043356C409A0D30823AFA16F60B00B8BCE98BB37EB24A8258823D6B11F157&List=03e8ea21-64e6-4d37-8235-04fb61e122e9&RootFolder=/publications/AGARD/AGARD-R-783

Anderson, D. F., & Eberhardt, S. (2010). Understanding flight. New York, NY: McGraw-Hill.

Bower, A. & Xu, J. (2019). EN0040: Dynamics and Vibrations, notes [2.1 Forces]. Retrieved from https://www.brown.edu/Departments/Engineering/Courses/En4/Notes/Forces/Forces.htm#Sect21

Bueno Tintoré, I. (2018). *Design of a three-axis wind tunnel force balance* (Undergraduate thesis). Retrieved from https://urn.nsk.hr/urn:nbn:hr:119:249595

Gonzalez, M., Ezquerro, J. M., Lapuerta, V., Laveron, A., & Rodriguez, J. (2011). Components of a wind tunnel balance: Design and calibration. In J. C. Lerner (Ed.), *Wind tunnels and experimental fluid dynamics research.* InTech. https://doi.org/10.5772/21095

Post, S., & Morris, M. (2010, June). *Force balance design for educational wind tunnels.* ASEE Annual Conference, Louisville, KY.

Reynolds, R. S. (2005). Application of low speed wind tunnels in teaching basic aerodynamics. *Journal of Aviation/Aerospace Education & Research, 14*(2). Retrieved from https://commons.erau.edu/jaaer/vol14/iss2/6

Ribeiro, S. K., Kobayashi, S., Beuthe, M., Gasca, J., Greene, D., Lee, D. S., . . . Zhou, P. J. (2007). *Transportation and its infrastructure.* Retrieved from University of California, Davis, Institute of Transportation Studies website https://escholarship.org/uc/item/98m5t1rv

Rigby, K. T. (2015). Real-time computer-based simulation as an intervention in aerodynamics education. *Journal of Aviation/Aerospace Education & Research, 24*(2). https://doi.org/10.15394/jaaer.2015.1634

Robinson, M., Schramm, J. M., & Hannemann, K. (2007). An Investigation into Internal and External Force Balance Configurations for Short Duration Wind Tunnels. Notes on Numerical Fluid Mechanics and Multidisciplinary Design (NNFM) New Results in Numerical and Experimental Fluid Mechanics VI, 96, 129-136. https://doi.org/10.1007/978-3-540-74460-3_16

Vadassery, P. (2012). *Design, calibration and testing of a force balance for a hypersonic shock tunnel.* Retrieved from The University of Texas at Arlington website http://adsabs.harvard.edu/abs/2012PhDT.........9V